



ELSEVIER

Palaeogeography, Palaeoclimatology, Palaeoecology 184 (2002) 131–146

PALAEO

www.elsevier.com/locate/palaeo

Reconstructing daily temperatures from growth rates of the intertidal bivalve mollusk *Chione cortezi* (northern Gulf of California, Mexico)

Bernd R. Schöne^{a,*}, Jocelina Lega^b, Karl W. Flessa^a, David H. Goodwin^a,
David L. Dettman^a

^a Department of Geosciences, The University of Arizona, Tucson, AZ 85721, USA

^b Department of Mathematics, The University of Arizona, Tucson, AZ 85721, USA

Received 25 October 2001; accepted 11 February 2002

Abstract

We establish a model for the reconstruction of average daily sea surface temperatures from calcification rates of an intertidal bivalve mollusk. The rate of shell production in *Chione cortezi* (Carpenter, 1864, ex Sloat MS) is mainly controlled by water temperature, ontogenetic age and the effect of tidal cycles. Statistical methods developed by dendrochronologists can successfully extract the water temperature signal from daily growth increment chronologies. After removal of noise, the growth rates are expressed as scaled daily growth indices. Average daily water temperatures during the first half of the year are highly correlated with the scaled daily growth index values of recent and subrecent specimens, using the multi-valued function presented here. Increment width analysis can reconstruct daily average water temperatures with a mean error of less than 3%. This technique provides an independent method for reconstructing temperatures in fossil specimens of species with living representatives and can supplement high-resolution temperature reconstructions based on geochemical analysis. © 2002 Elsevier Science B.V. All rights reserved.

Keywords: growth rate; $\delta^{18}\text{O}$; growth index; sclerochronology; paleoecology

1. Introduction

Detailed reconstructions of seasonal temperature changes can be vital in developing and testing models of ancient climate variation (e.g., Kutzbach and Guetter, 1986; Kutzbach et al., 1993). Although tree-ring analysis has provided extra-

ordinarily precise climatic reconstructions in the terrestrial realm for the last 1500 yr of climate history (e.g., Briffa et al., 1996), many of the statistical methods of dendrochronology (for a review see Cook and Kairiukstis, 1990) have not been extensively applied to the analysis of growth increments in the hard parts of marine organisms. This is despite the well-known role of temperature in calcification rates of bivalve mollusks (e.g., Davenport, 1938; Gunter, 1957; Berry and Barker, 1968). Typically, growth rate increases

* Corresponding author.

E-mail address: bernd.schoene@excite.com (B.R. Schöne).

with rising water temperatures (e.g., Koike, 1980; Kennish and Olsson, 1975). However, many other environmental and physiological conditions also control growth rates, for example, age (von Bertalanffy, 1934), tidal cycle (Evans, 1972) and day/night cycles (Clark, 1975). Due to the complex interaction of these growth controls, it is often difficult to reconstruct a specific environmental parameter from growth increment width data. This might be one reason why geochemical techniques have become the most common method for environmental reconstructions using accretionary skeletons. Although a few studies have successfully correlated annual temperatures to the annual growth increment widths of bivalve mollusks (Jones et al., 1989: for *Mercenaria mercenaria* (Linné); Marchitto et al., 2000: for *Arctica islandica* (Linné)), no attempts have yet been made to infer daily water temperatures from variation in growth increment widths in bivalve mollusks.

In the present study, we determine if variation in daily growth rates in a bivalve mollusk can be used to reconstruct daily water temperatures. The intertidal bivalve mollusk *Chione cortezi* (Carpenter, 1864, ex Sloat MS) is particularly abundant in the northern Gulf of California. Previous studies revealed that temperature, age and tidal cycle explain most of the variability in the growth patterns of this species:

1. Growth occurs only in temperatures between about 15 and 31°C, with highest growth rates confined to water temperatures of about 24°C (Goodwin et al., 2001; Schöne et al., 2002).
2. The effect of ontogenetic age on the growth rate is expressed as decreasing annual increment widths from the umbo to the commissure (Schöne et al., 2002).
3. One increment of shell material is formed every 24.8 h (1 lunar day). This periodic accretion enables us to use growth increment counts for exact dating of each portion of the shell. Daily growth increments that form during neap tides are larger than those produced during spring tides. As a result of this cyclic change in increment width, a fortnightly growth pattern emerges (Schöne et al., 2002). We apply statistical methods developed by den-

drochronologists to extract daily water temperatures from variation in growth increment widths in live-collected shells. Calibration with satellite-derived temperatures, in situ temperature logger data, and oxygen isotope data are used to test the strength of this inexpensive and rapid method for temperature reconstruction based on variations in calcification rates. We demonstrate the applicability of increments width analysis (IWA) by examining shells that have also been sampled for variation in oxygen isotope ratios.

2. Materials and methods

Our study area is located at the lower Colorado River delta in the northern Gulf of California (Fig. 1). Before the diversion of the Colorado

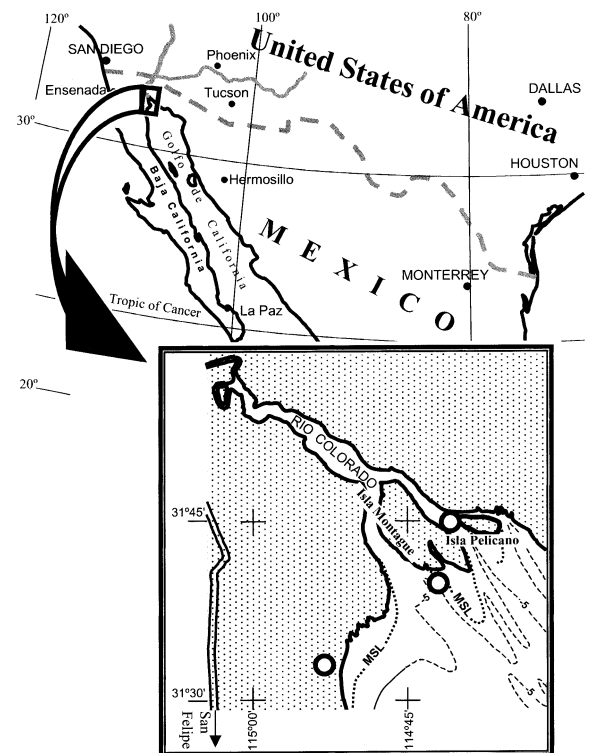


Fig. 1. Sample localities (open circles) in the Northern Gulf of California region. Samples were taken in mid-intertidal at low tide from Isla Montague (N 31°40.22, W 114°41.41) and Isla Pelicano (N 31°45.70, W 114°41.72). Subrecent specimens were taken from a high intertidal chenier at North Island (N 31°34.20, W 114°53.00).

River and the construction of upstream dams in the 1930s, large amounts of freshwater were delivered to this region. Today only a trickle reaches the delta, and normal marine conditions prevail (Lavín and Sánchez, 1999). The tidal regime is semidiurnal with a mean range of about 5 m. The study area is characterized by hot and dry conditions: monthly air temperatures exceed 32°C in summer and precipitation rates are low (annual mean is about 60 mm; Hastings, 1964).

2.1. Daily sea surface temperatures (SSTs)

Daily SSTs for the sample area were obtained from satellite measurements (<http://www.cdc.noaa.gov/>). Every 29th SST value was omitted in order to correct for lunar days, because a lunar day exceeds a solar day by approximately 50 min in length. The spatial resolution of these datasets is 14 km². Local temperatures – where the bivalve mollusks actually grew – were recorded by a HOBO Temp[®] temperature logger in a waterproof container chained to a concrete anchor at Isla Montague (N 31°40.22, W 114°41.41). The logger recorded the temperature to the nearest 0.5°C every 2 h from February 16, 1999 to February 16, 2000 (see Goodwin et al., 2001, for a detailed description; Fig. 2a). Lunar day temperatures were calculated from temperature logger data (Fig. 2a). Each of the lunar day temperature time-series was fitted with a fifth degree polynomial in order to obtain a smooth curve of intra-annual lunar day temperatures (Fig. 2a–c). This effectively removes high-frequency fluctuations and the influence of tidal cycles from the temperature time-series.

2.2. Sample material, preparation and measurements

We collected three living specimens of the in-faunal bivalve *Chione cortezi* at low tide from the mid-intertidal zone at two localities on the Colorado Delta. One 7-yr-old (based on counts of annual growth increments) specimen was obtained from Isla Pelicano (IP1-A1R; N 31°45.70, W 114°41.72) in November 1995 and two 3-yr-old specimens on February 16, 2000 from Isla Mon-

tague (IM11-A1R and IM11-A2R; N 31°40.22, W 114°41.41) – the same position as the temperature loggers. We also analyzed two subrecent *C. cortezi* shells (5-yr-old NI1-D6 and 11-yr-old NI2-D119) from North Island (N 31°34.20, W 114°53.00) collected in November 1996. Amino acid racemization dating (Kowaleski et al., 1998) reveals that specimen NI1-D6 was alive between 1450 and 1500 AD and specimen NI2-D119 between 1100 and 1150 AD.

The flesh was removed from the living shells immediately after collection to prevent further shell deposition. After coating with epoxy resin, one valve of each specimen was cut along the axis of maximum growth using a low-speed (Buehler Isomet) saw. Both halves were ground on glass plates (600, 800 and 1000 grit powder) and polished on laps (9, 6 and 0.3 µm).

One half of each cross-sectioned and polished valve was etched in a NaOH-buffered EDTA solution (0.25 M, pH 7.9) for 1–2 h, rinsed in water and acetone, allowed to air-dry and coated with a 30-nm Au–Pd layer. Etching and coating increased the contrast of the growth increments. A caliper was used to measure the distances (to the nearest 20 µm) between major growth lines (i.e., between the annual increments) in radial cross-sections using a reflected light binocular microscope. In addition, the cross-sections were viewed under a reflected light microscope (magnification 100×) and digitized with the image capture software Optimas version 5. Daily increment widths (ranging from a few µm to 300 µm thickness) of all specimens were measured to the nearest 1 µm with Scion/NIH version 3b image analysis software (available at <http://www.scioncorp.com>). We measured daily increments of the third year of growth (i.e., between the second and third winter break) of the live-collected specimens in order to compare growth rates at similar ontogenetic ages in different specimens. In both subrecent specimens daily growth rates were estimated from fortnightly increments. We measured the width of fortnightly increments of the third annual increments in specimen NI1-D6 and the fourth annual increment in specimen NI2-D119 in order to compare growth rates in specimens of different ontogenetic ages.

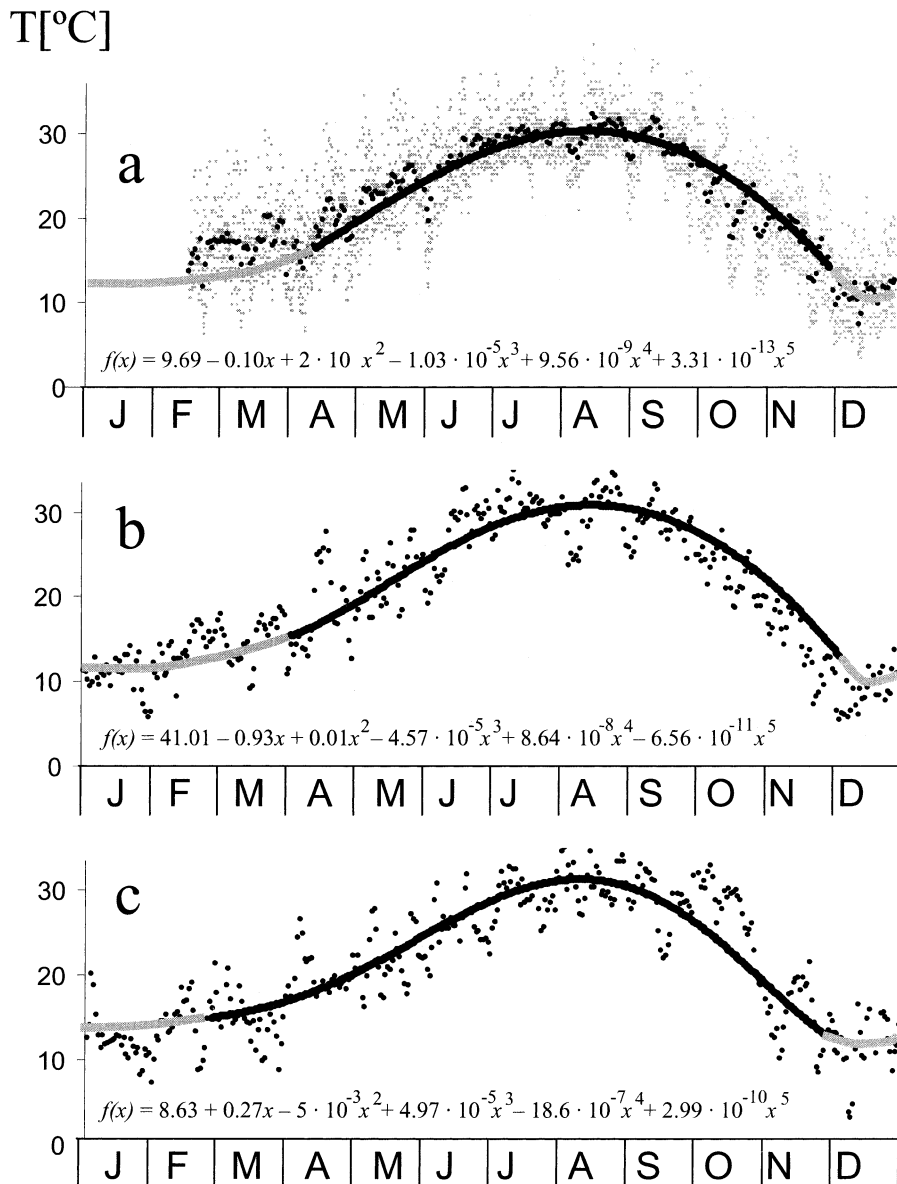


Fig. 2. Lunar day SSTs (black dots) in the study area. Fifth degree polynomials on daily increments provide ‘filtered’ daily temperatures. (a) Temperature logger data (grey dots) were measured every two h beginning from February 16, 1999. Also shown are calculated average lunar day temperatures and polynomial fit. (b) Daily water temperatures from satellite measurements over the period January–December 1999. (c) Daily water temperatures from satellite measurements over the period January–December 1991.

2.3. Oxygen isotope analysis and temperature reconstruction from oxygen isotopes

For oxygen isotope analysis the other half of each polished valve was rinsed several times ultra-

sonically with deionized water prior to sampling. The outer shell layer (prismatic layer) was sampled using a 300- μ m drill under a binocular microscope. Five to 16 microsamples were taken from each shell. Each of the 54 drill holes yielded

50–200 μg of carbonate for isotopic analysis. A Finnigan MAT 252 equipped with a Kiel III automated sampling device was used to process the samples. $\delta^{18}\text{O}$ is reproduced relative to PDB on a NBS-19 value of -2.20‰ . Precision is better than 0.1‰ .

Oxygen isotope-derived temperature estimates are based on Grossman and Ku's (1986) equation for biogenic aragonite. We have rewritten their paleothermometry relationship so that all water values derived from this equation are corrected to the SMOW scale:

$$T (^{\circ}\text{C}) = 20.6 - 4.34 (\delta^{18}\text{O}_{\text{aragonite}} - (\delta^{18}\text{O}_{\text{water}} - 0.2)).$$

A 1‰ shift in $\delta^{18}\text{O}$ of the shell carbonate results from a temperature change of 4.7°C .

2.4. Data analysis

The model presented in this study will be illustrated by an intra-annual daily growth increment time-series of *Chione cortezi* (IP1-A1R) from the mid-intertidal zone of the northern Gulf of California (Fig. 3a).

2.4.1. Filtered daily growth data: removing tidal cycles and other 'noise'

Fourier-transformed raw growth increment data reveal cyclic growth patterns (Fig. 3b; Dolman, 1975). Even though the Fourier plot is symmetric with respect to the y -axis (which is to be expected, because the data consist of real numbers), we represent the central part of the Fourier spectrum, for wave numbers between -0.8 and $+0.8$. Two clusters near $k = \pm 0.49$ and $k = \pm 0.43$ correspond to a period $\tau = 2\pi/|k|$, approximately equal to 13 and 14.5 lunar days (fortnight periods), respectively. Other peaks of lower amplitude than the tidal cycles are here considered as 'noise' and reflect minor variation in daily growth increments. The large peak near the origin represents low-frequency oscillations and contains information related to large-scale (seasonal) variability of daily growth. These parts of the spectrum can be extracted from the time-series by isolating (filtering) each region in Fourier space (Fig.

3b) and Fourier-transforming it back to real space (Fig. 3c,d). The curve labeled 'Tidal oscillations' in Fig. 3c corresponds to the inverse Fourier transform of the two clusters with the same label in Fig. 3b (other Fourier modes are set to 0). The envelope of the tidal oscillations curve in Fig. 3c was obtained by shifting one of the clusters corresponding to tidal oscillations to the origin of Fourier space, applying an inverse Fourier transform to it, and multiplying the result by two (since $\cos(kx) = 1/2(e^{ikx} + e^{-ikx})$, the amplitude of oscillations in real space is twice as big as the amplitude of each of the corresponding modes in Fourier space). Extraction of the effect of tidal cycles and minor fluctuations in growth reveals the general growth pattern, which we term 'filtered daily growth data'. The curve labeled 'filtered growth' in Fig. 3d is indeed the inverse Fourier transform of the center peak ('Low frequency oscillations', Fig. 3b) of the Fourier-transformed raw growth data.

2.4.2. Age-trend modeling: exponential model

The effect of aging on growth in *Chione cortezi* is obvious in the decrease of annual increment width with increasing ontogenetic age (Fig. 3e). The increase in shell length $L(t)$ at time (t) can be modeled by means of the following differential equation:

$$\frac{dL}{dt} = -k(L - L_{\infty}),$$

where L_{∞} is the asymptotic length of the shell and k is a growth constant. In what follows, we measure time in years and lengths in microns. This model, similar to Newton's law of cooling and known as the von Bertalanffy equation (von Bertalanffy, 1938), indicates that the rate of change in the length of the shell is directly proportional to the difference between the current length L and its asymptotic value L_{∞} . The above differential equation can be integrated to give

$$L(t) = L_{\infty} + (L(T) - L_{\infty}) \exp(k(T - t)),$$

where $L(T)$ is the length of the shell at some reference time T (in what follows, we use $T = 2$ yr,

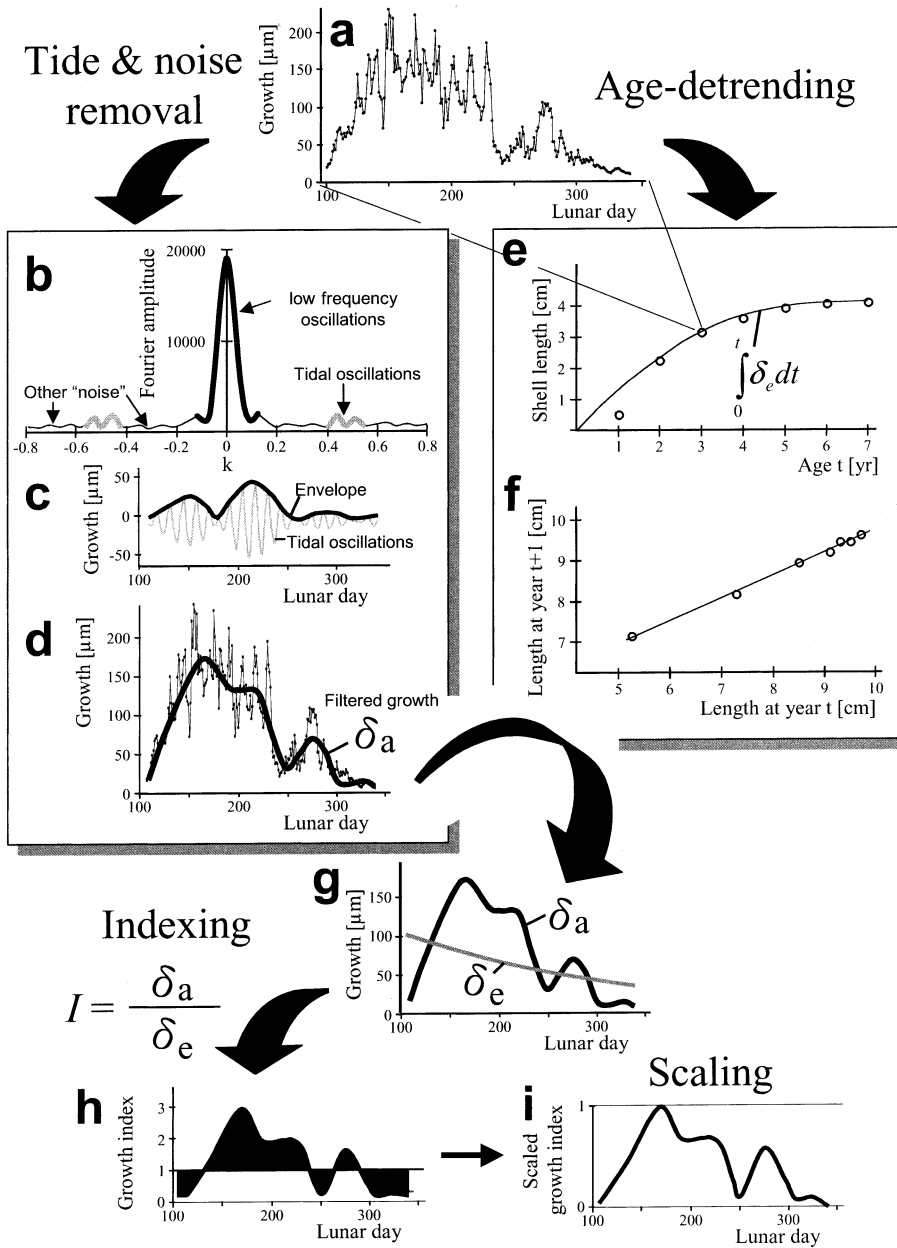


Fig. 3. Data analysis. (a) Intra-annual lunar day growth increment width time-series of a 3-yr-old *Chione cortezi*. (b) Fourier transform of the time-series depicted in (a). The frequency clusters include low-frequency oscillations, tidal oscillations and other ‘noise’. (c) The tidal oscillations from (b) are back transformed into real space. (d) The low-frequency oscillations (b) are superimposed in real space on the raw growth data (a). Low-frequency oscillations are also termed ‘filtered growth’. (e) Annual increment widths (open circles) and exponential fit. (f) The coefficients for the exponential model in (e) are found by the Ford–Walford plot (length of the shell at time t versus length of the shell at time $t+1$, where $t = \text{yr}$). The exponential curve in (e) and the linear fit in (f) is the predicted growth. (g) The filtered intra-annual growth curve (d) and the predicted intra-annual growth curve are depicted. (h) Indexing: daily growth indices were obtained by dividing filtered daily growth data by predicted daily growth data. (i) Growth indices from (h) were scaled, so that the no growth equals 0 and highest growth rate 1. (j) Scaled growth indices of the first half of the year from reference specimens are plotted as a function of temperature and fitted with polynomials. In some cases the best fit of the data is achieved by fitting portions of the growth data individually with different functions. This model gives water temperatures for specific scaled growth indices.

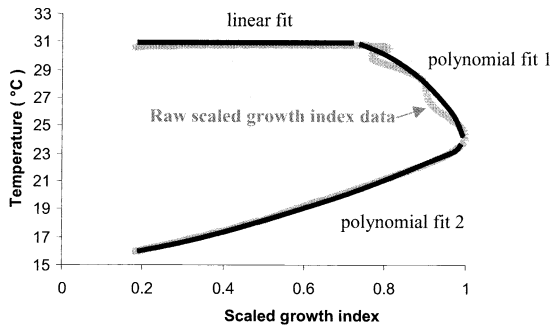


Fig. 3j (Continued).

because the growth period during the birth year is shorter than during subsequent years and the first annual increment is therefore incomplete). This expression implies that the length of the shell t_0 yr after time t , namely $L(t+t_0)$, is a linear function of $L(t)$, the length of the shell at time t . More precisely, we have

$$\begin{aligned} L(t+t_0) &= L_\infty + (L(T)-L_\infty) \exp(k(T-t)-kt_0) \\ &= L_\infty + (L(T)-L_\infty) \exp(k(T-t)) \\ &\quad \exp(-kt_0) \\ &= [L_\infty + (L(T)-L_\infty) \exp(k(T-t))] \\ &\quad \exp(-kt_0) + L_\infty(1-\exp(-kt_0)) \\ &= a L(t) + b. \end{aligned}$$

where $a = \exp(-k t_0)$ and $b = L_\infty (1-a)$. The coefficients a and b can be found by linear regression from the Ford–Walford plots (Walford, 1946; Bauer, 1992) giving the shell length at $t+t_0$ as a function of the shell length at t (Fig. 3f). The parameters L_∞ and k are then obtained from a and b using the following formulas

$$L_\infty = \frac{b}{1-a}; \quad k = \frac{1}{t_0} \ln(a).$$

Predicted daily growth δ_e (Fig. 3g) is obtained from the exponential model by taking the derivative of the length of the shell with respect to time, where time is now expressed in lunar days (1 lunar day = 24.8 h). Because there are approximately 353 lunar days in an Earth year, we have

$$\begin{aligned} \delta_e &= \frac{dL}{dt} \\ &= \frac{d}{dt} \left[L_\infty + (L(T)-L_\infty) \exp \left(k \left(T - \frac{1}{353} \right) \right) \right] \\ &= (L_\infty - L(T)) \frac{k}{353} \exp \left(k \left(T - \frac{t}{353} \right) \right), \end{aligned}$$

where T is expressed in years and t is in lunar days. The parameters k and L_∞ are computed as described above.

In the case of fossil shells, for which growth increments are only available as averages over a period of τ days, increments δ_e are computed as the change in shell length over τ days, i.e., $\delta_e = L(t+\tau) - L(t)$.

2.4.3. Removal of the age trend and creation of dimensionless growth data

The variability in growth increment time-series of many organisms, including mollusks, is controlled by environmental parameters and physiological constraints. In order to resolve the environmental signals from growth rates, physiological growth components (e.g., the age-related growth trend) should be removed. In dendrochronology this method is known as age-detrending (Cook and Kairiukstis, 1990) and indexing (Fritts, 1976). First, the age-related growth trend is estimated by calculating a fitted curve to growth data (see 2.4.2. Age-trend modeling: exponential model). This curve is referred to as predicted growth. In a second step, the age trend is removed from the growth increment width time-series by indexing. Observed growth is divided by predicted growth. This gives dimensionless growth data, known as growth indices. Age-detrending and indexing is here applied to bivalve mollusk growth increment chronologies. Accordingly, daily growth indices I are computed by dividing the daily average growth increments δ_a (observed growth data, which are already corrected for the influence of the tides) by the predicted daily growth increments δ_e : $I = \delta_a / \delta_e$ (Fig. 3g,h). This effectively removes the influence of aging from average daily growth data.

In order to compare the daily growth indices of different specimens we scaled the daily growth

indices to their intra-annual maximum, so that scaled indices take values between 0 and 1, where zero means no growth and one means maximum growth (Fig. 3i). This is justified by the fact that the highest intra-annual growth rate in *Chione cortezi* is always related to the same water temperature, i.e., approximately 24–25°C (Goodwin et al., 2001; Schöne et al., 2002).

2.4.4. The model

Scaled daily growth indices of reference specimens are plotted against temperature (Fig. 3j). The data points are then fitted with polynomial functions. In some cases the best fit of the data is achieved by fitting portions of the growth data individually with different functions. This function (= model) gives water temperatures for specific scaled growth indices. It is multi-valued, because the same index values are observed for different temperatures on both sides of the optimal growth temperature. Temperature conditions can be estimated from scaled growth indices of other specimens using this reference model.

2.4.5. Errors on temperature predictions

Average relative errors on estimated temperature are calculated by computing the relative error E_r on temperature for each day,

$$E_r = \frac{|\text{estimated temperature} - \text{measured temperature}|}{\text{measured temperature}}$$

where $|x|$ represents the absolute value of x . The average of these values gives the relative error for a whole data set.

3. Results

3.1. Inter-annual growth pattern: age-trend

Annual increment widths decrease from the umbo to the commissure as *Chione cortezi* matures. This age-related growth trend is herein predicted with the exponential model. In all specimens studied here the agreement between the predicted and observed values is excellent

Table 1

Values of L_∞ and k for the shells discussed in this paper

Shell	L_∞ (μm)	k ($\mu\text{m}/\text{yr}$)
IP1-A1R	99 000	0.59
IM11-A1	93 500	0.54
IM11-A2	103 000	0.38
NI1-D6	53 099	0.647
NI1-D119	66 287	0.491

L_∞ is the predicted final shell length, the shells' average growth rate is given by the k value.

($R^2 > 0.964$). The parameters L_∞ and k (Table 1) for the exponential model were computed from Ford–Walford plots giving $L(t+t_0)$, as a function of $L(t)$, where $t_0 = 1$.

Different recent *Chione cortezi* specimens exhibit slightly different L_∞ values, i.e., varying predicted final shell lengths. In contrast, the theoretical shell length of subrecent *C. cortezi* specimens studied here is significantly smaller than that of recent shells. Relative growth rates (k values) do not reflect this difference. With the exception of specimen IM11-A2L the k values of recent and subrecent specimens remain in a relatively narrow range. The correlation between the relative growth rate k and the predicted final shell length L_∞ is poor ($R^2 = -0.28$).

3.2. Intra-annual growth patterns

All three living *Chione cortezi* specimens used in this study show very similar intra-annual growth patterns (Fig. 4). The general growth patterns in *C. cortezi*, including the influence of tidal cycle on growth, were described by Goodwin et al. (2001) and Schöne et al. (2002). Growth starts in February or March after a winter shutdown. After maximum growth rates in late May and early June (300 $\mu\text{m}/\text{lunar day}$), the production of shelly material drops sharply towards July or August (5–10 μm). Growth rates increase again and reach another peak in the fall. Thereafter the calcification rates decrease towards the coldest season of the year. No shell production occurs from late December through February or March. The subrecent specimens show similar intra-annual growth profiles. In the absence of direct observations,

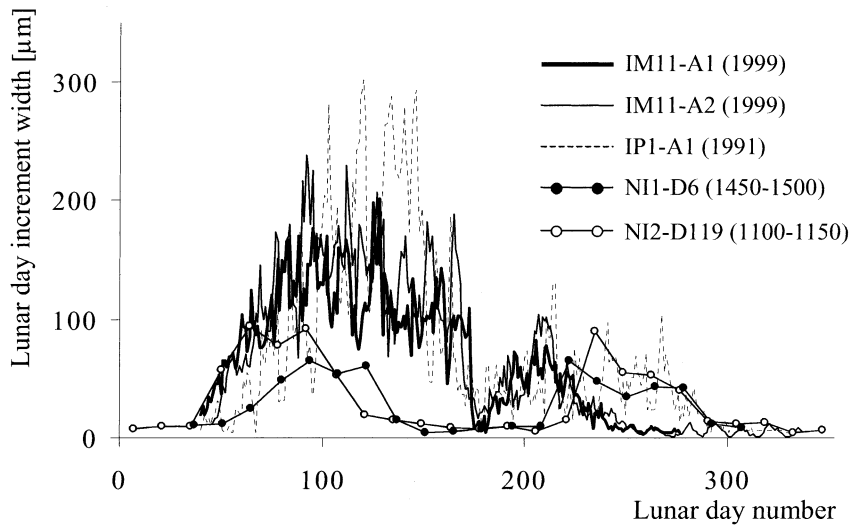


Fig. 4. Intra-annual growth (third year of growth in Recent shells and NI1-D6, fourth year of growth in NI2-D119) from all five *Chione cortezi* specimens studied here. Lunar day increment widths were obtained from the live-collected specimens (IM11-A1R, IM11-A2R and IP1-A1R). For subrecent specimens only fortnight increment widths were measured.

only relative dates can be assigned to the lunar day growth increments. For visual comparison of intra-annual growth rates, the curves of all specimens were shifted so that the minimum growth rates in the hot summer overlap and are thus assumed to occur on the same date.

3.3. A model for water temperature prediction from scaled daily growth indices

Similar numbers of daily increments were counted in the third year (growth during 1999) of both specimens collected alive at Isla Mon-

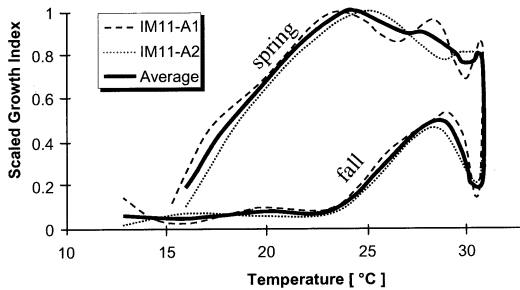


Fig. 5. Scaled growth indices (growth during 1999) from *Chione cortezi* specimens collected alive at Isla Montague are depicted as a function of temperature (filtered temperature logger data). An average of both shells is also shown.

tague (292 increments in IM11-A1L and 286 increments in IM11-A2L; Fig. 4). Both specimens grew next to each other and were exposed to virtually the same environmental conditions. Previous studies have shown that temperature is the most important control on growth rate in *Chione cortezi* (Goodwin et al., 2001; Schöne et al.,

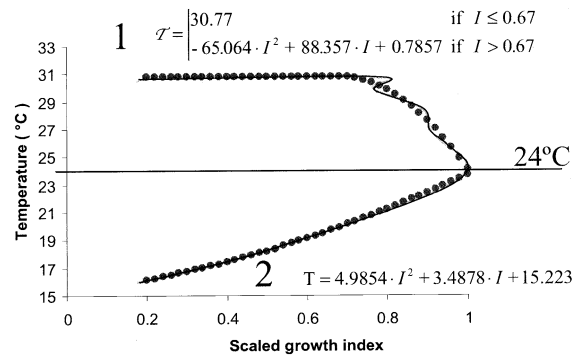


Fig. 6. Filtered water temperatures are depicted as a function of the average scaled lunar day growth curve from Fig. 5. The data points were fitted with a multi-valued function. This function allows the reconstruction of daily water temperatures from scaled growth indices. The horizontal line marks the optimal growth temperature and the maximum growth rate. Below this line (at lower than optimal growth temperatures) temperature reconstruction uses function 2, above this line function 1.

2002). Thus, in Fig. 5 scaled daily growth increments of these specimens are plotted as functions of temperature (temperature logger data fitted with a fifth degree polynomial), together with an average scaled daily growth increment curve. Both specimens show an almost identical growth behavior at similar temperatures. Skeletal material is produced when temperatures exceed 13°C. Maximum growth rates (growth index = 1) occur at about 24°C (= optimal growth temperature). Low growth rates were observed during highest temperatures (= summer minimum).

The average growth curve of specimens IM11-A1R and IM11-A2R is used here to establish a model for the reconstruction of sea surface water

temperatures from growth rates. The upper branch of the average curve in Fig. 5 corresponds to growth during the first half of the year until the summer growth minimum. Growth between the hot summer and the following winter is represented by the lower branch of the curve. During the second half of the year maximum growth rates are lower. Maximum growth rates during late summer and fall barely exceed 50% of the spring growth maximum.

The first half of the average lunar day growth curve can be isolated and used to plot daily water temperature (temperature logger data) as a function of scaled growth indices. This multi-valued function is shown in Fig. 6. The bottom branch

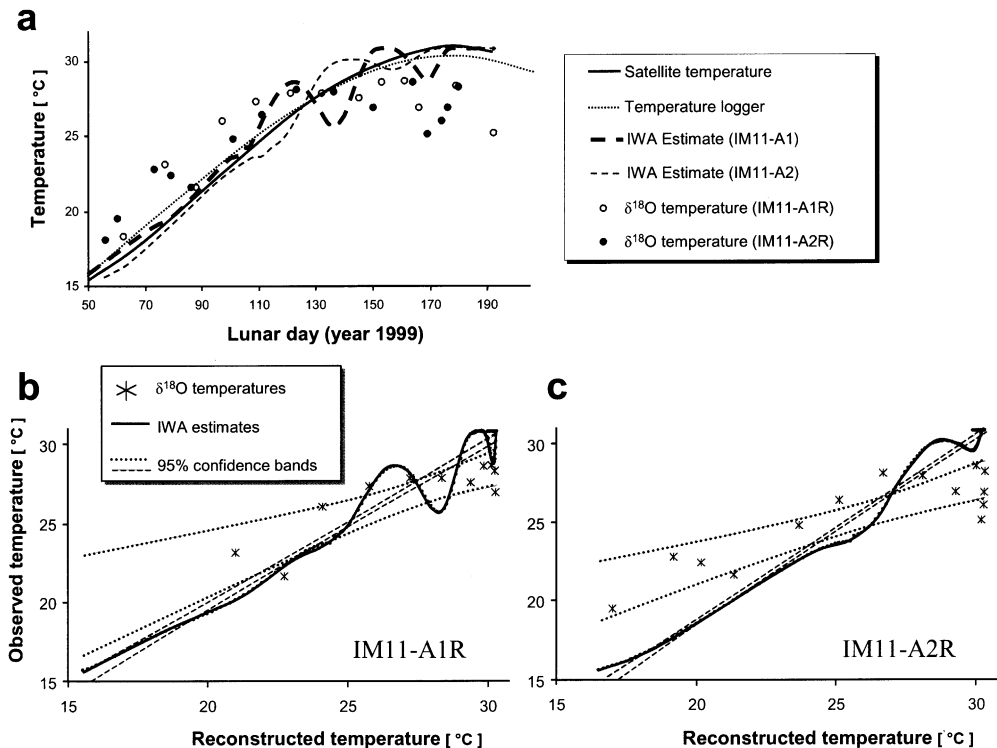


Fig. 7. (a) Measured (1991) and reconstructed daily temperatures from specimens IM11-A1R and IM11-A2R are superimposed. Temperature logger data and satellite-derived SSTs are almost identical. Temperatures predicted by IWA fluctuate slightly around the observed data, but the relative error between predicted and measured temperatures is as low as 3%. Growth temperatures are estimated from oxygen isotope values. These tend to be lower than measured or IWA-predicted daily temperatures during the hot summer and higher during the early spring (see text for discussion). Comparison of temperature reconstructions based on scaled growth indices and oxygen isotope ratios, 95% confidence bands are given by thin dotted lines for both prediction methods. The confidence bands of temperatures predicted from IWA and oxygen isotope ratios overlap at the optimal growth temperature range (about 25°C) in both shells IM11-A1R (b) and IM11-A2R (c).

(corresponding to temperatures below the optimal growth temperature) of this plot can be approximated by a quadratic function:

$$T = 4.9854 \cdot I^2 + 3.4878 \cdot I + 15.223,$$

and the top branch (corresponding to temperatures above the optimal growth temperature) by a straight line and a quadratic function. The equation for the two sections of the top branch is given below:

$$T = \begin{cases} 30.77 \text{ if } I \leq 0.67 \\ -65.064 \cdot I^2 + 88.357 \cdot I + 0.7857 \text{ if } I > 0.67 \end{cases}$$

Points corresponding to the above formulas are plotted in Fig. 6. In the following section, we use this function to predict water temperature from scaled daily growth indices for one recent and two subrecent shells.

3.3.1. Comparing different temperature datasets

Estimated temperatures from scaled growth indices of IM11-A1R and IM11-A2R fluctuate slightly around the satellite SST curve (Fig. 7a). The deviations of the predicted temperatures from measured temperatures are particularly high between 25 and 30°C. The mean relative temperature error (predicted temperature versus measured SST) for IM11-A1R is 2.91% and 2.20% for IM11-A2R. Our model is based on temperature logger data measured at the position where specimens IM11-A1R and IM11-A2R grew. For comparison, Fig. 7a also shows daily temperatures based on satellite measurements (fifth degree polynomial fit) and temperatures reconstructed from oxygen isotope values of the shells (IM11-A1R and IM11-A2R). The temperature profiles from satellite and ground measurements closely resemble each other. Temperatures derived from oxygen isotope values correspond to temperature logger data during March through June, but they are on average 2–3°C lower than temperature logger data during July and August. In Fig. 7b,c temperature predictions based on oxygen isotope ratios and daily growth rates (of IM11-A1R in (b) and

IM11-A2R in (c)) are plotted against observed temperatures including the 95% confidence levels. The confidence bands for IWA and $\delta^{18}\text{O}$ overlap at the optimal temperature range (at about 25°C).

3.4. Testing the model I: estimating water temperature from scaled growth indices of a recent shell

We apply the model described in 3.3. A model for water temperature prediction from scaled daily growth indices to estimate water temperatures from growth data of a *Chione cortezi* specimen from Isla Pelicano (IP1-A1R). Based on our previous work (Goodwin et al., 2001), we assume that growth does not stop during the hot summer, minimum summer growth occurs at highest temperatures and that maximum growth rates occur at the same optimal growth temperature of about 24°C. The third annual increment of specimen IP1-A1R was deposited during 1991. Fig. 8 shows the observed water temperature, based on daily satellite measurements, and the temperature predicted by the above formula (solid dark gray curve) for the first part of year 1991. In addition, water temperatures, reconstructed from oxygen isotope data of the shells, are depicted. The agreement between daily SSTs and predicted daily water temperature is very good except for temperatures between about 26 and 30°C. $\delta^{18}\text{O}$ -derived

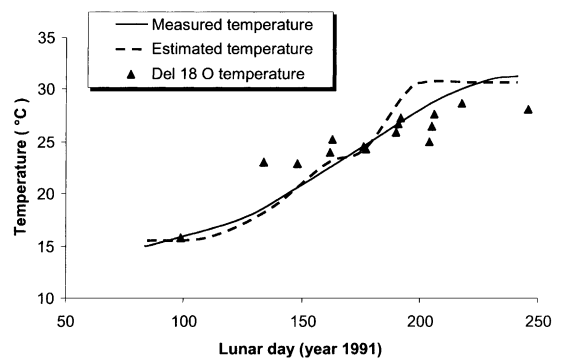


Fig. 8. The model tested on shell IP1-A1R. Predicted and observed temperatures during 1991. Predicted temperatures fluctuate slightly around the observed temperatures with a relative error of 2.83%. Oxygen isotope derived temperatures are higher than observed during early spring and lower during hot summer. For explanation see Fig. 7 and text.

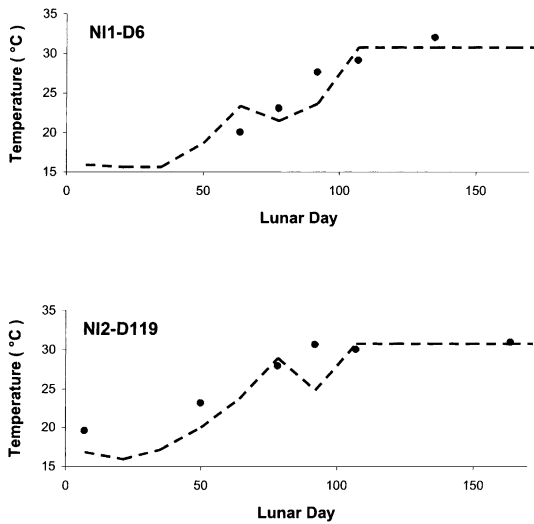


Fig. 9. The model tested on subrecent shells. The only available independent temperature data are those estimated from oxygen isotope data (dots). Temperatures predicted from IWA and temperatures derived from oxygen isotope values are similar.

water temperatures closely resemble predicted water temperatures during March through June, but are lower than predicted or measured temperatures in July and August, again. The relative temperature error for IP1-AR1 is 2.83%.

3.5. Testing the model II: estimating water temperature from scaled growth indices of subrecent shells

Finally, we apply the model to estimate water temperatures from scaled growth indices of two subrecent *Chione cortezi* specimens from North Island (growth during age four for NI2-D119 and growth during age three in NI1-D6). Estimated temperatures are compared to temperatures derived from oxygen isotopes (Fig. 9). Both reconstructed temperature curves are in good agreement. The number of data points is, however, too low to provide a statistical value for the goodness of fit.

4. Discussion

Mollusks and other organisms with accretion-

ary hard parts serve as biological archives of environmental conditions (Neville, 1967; Jones, 1996). Bivalve mollusk growth is especially sensitive to slight environmental changes (Pannella and MacClintock, 1968; Koike, 1980). This sensitivity is reflected in slight variations of growth rates and in geochemical properties of the shell. Many recent paleoenvironmental studies rely almost completely on geochemical analysis of the shells (Kobashi and Grossman, in press) or use sclerochronological methods only to assign dates to sampled portions of the shells (e.g., Kirby et al., 1998; Steuber, 1996). Other possible applications of sclerochronology have been largely neglected, namely the potential of IWA for environmental reconstructions.

4.1. Problems and limitations of IWA for temperature reconstructions

Our model does not provide a perfect fit between reconstructed and observed daily temperatures. Despite the removal of age- and tidal cycle-related growth trends, some remaining variation in the growth rates is not explained by temperature variation. The departures from a perfect fit are especially relatively high between temperatures of about 25–29°C and exhibit some low-frequency oscillation (e.g., Fig. 7). The reason for this pattern is not clear. Factors other than temperature seem to control the calcification rate to a greater extent during this time of the year. Cycles induced by spawning may be one possible explanation for this variation. Schöne et al. (2002) observed spawning breaks in about June in *Chione cortezi*. This is about the time when temperatures rise above 25°C.

IWA temperature reconstruction is limited to the first half of the year. Whereas growth during spring and early summer is highly correlated with water temperature, there is much less coincidence between growth rates and temperature during the second half of the year. Nutrient deprivation in the late summer and fall may cause diminished growth rates. Shipboard measurements indicate a significant drop in phytoplankton concentrations at the end of the summer in the northern Gulf of California (Millán-Núñez et al., 1999).

Further investigation is needed to verify the role of nutrient availability on growth rates. This could refine our model.

Our model requires calibration of daily growth rates in living specimens with temperatures. It is, however, not clear if growth rates in *Chione cortezi* everywhere are controlled in exactly the same way. At other localities, or at other times, fluctuations in salinity or other environmental parameters could be higher. This could have an influence on growth rates. Therefore, recalibration is advised if *Chione* specimens from other localities are intended for IWA temperature reconstruction. Similarly, the reconstruction of daily temperatures using IWA in fossil bivalve mollusks requires the assumption that growth rates in fossils were controlled by the same growth parameters that were observed for extant specimens.

Scaling of growth indices requires that the growth rates decrease in the hot summer. Therefore, exact water temperatures can only be reconstructed from scaled growth indices if the intra-annual growth profile shows at least two growth peaks, one in late spring and another one later in the year. If the optimal growth temperatures are not reached within 1 yr, only one growth peak would be produced. This growth peak would be the highest relative growth rate within this year and would equal a scaled growth index of one. This peak would then – by definition – indicate a temperature of 24°C. In such cases, oxygen isotope analysis can help to recalibrate the growth index time-series.

Finally, we cannot assign precise calendar dates to reconstructed lunar day temperatures, because we do not know the exact date that growth started. Furthermore, our assumption, for cross-dating purposes, that the minimum summer growth occurs on the same day (the hottest day) each year, also introduces dating error. Only detailed studies of temperature records will establish the exact error introduced by these practices, but we judge that the error is likely to be less than 30 days.

4.2. Strength of IWA for temperature reconstructions

Once calibrated with temperatures, scaled daily

growth indices of *Chione cortezi* from the northern Gulf of California can predict water temperatures in the first half of the year with a temporal resolution of 1 day. IWA temperature reconstruction is less expensive than oxygen isotope analysis, a large number of daily growth increments can be measured and mathematically transformed in a short period of time, and only a standard computer is required.

Comparison of the two methods (Fig. 7b,c) suggests, at first glance, that IWA produces a better estimate of temperature than oxygen isotope analysis. The confidence intervals of the IWA estimates are much smaller than those based on $\delta^{18}\text{O}$ values: the mean error of temperature reconstruction using IWA is less than 3%. To some extent this is simply a consequence of the far greater sample size used in IWA. However, perhaps the most important difference in the two predicted vs. observed curves is the slope of the line. IWA produces a steeper slope than $\delta^{18}\text{O}$ analysis in both shells. $\delta^{18}\text{O}$ analysis predicts warmer temperatures during the colder part of the growth range and cooler temperatures during the hotter part of the growth range. Near the optimum growth temperature, the estimates are similar.

The differences in the slopes of the reconstructed temperature time-series (IWA and $\delta^{18}\text{O}$, respectively) could be reproduced by slight changes in the isotopic composition of the seawater during the year. Fresher waters in spring could have produced slightly elevated $\delta^{18}\text{O}$ -based temperature estimates, whereas saltier waters in summer could have reproduced slightly cooler $\delta^{18}\text{O}$ -based temperature estimates.

Another interpretation is based on the timing of daily growth during different seasons of the year. Goodwin et al. (2001) suggested that the tendency for $\delta^{18}\text{O}$ -based temperature estimates to predict warmer than actual temperatures in the colder part of the growth range but cooler than actual temperatures in the hotter part of the range was the result of varying growth rates within the daily temperature cycle. In the cool spring, growth is likely faster during the warmer day than it is during the cool night. As a result, the $\delta^{18}\text{O}$ values are biased toward the relatively

warmer daytime temperatures because more shell material is deposited then. Above the optimum growth temperature, more growth probably occurs during the cooler night than during the hotter day. As a result, the $\delta^{18}\text{O}$ values are biased toward the relatively cooler nighttime temperatures.

Thus, the difference in slope is likely a consequence of the fact that $\delta^{18}\text{O}$ values are affected by the varying amounts of shell material deposited under different growth. Temperatures closer to the growth optimum are, in a sense, over-sampled, while increment widths can be directly calibrated with ambient water temperatures and are thus less biased.

IWA, therefore, is likely a more sensitive indicator of temperature variation in the environment than oxygen isotope analysis. Although neither method can predict temperatures above or below the individual's growth range, oxygen isotope analysis will tend to underestimate the growth range simply because the samples of shell material are likely to be volumetrically biased toward the optimum part of the range.

4.3. Strength and limitations of geochemical methods for temperature reconstructions

There are two major advantages of temperature reconstructions from oxygen isotopes: (1) temperature reconstruction is not limited to the first half of the year and (2) the method does not require calibration with living specimens. The influence of the geographic position on the fractionation of the oxygen isotopes is known and can be modeled (Broecker, 1989). Therefore, $\delta^{18}\text{O}$ derived temperatures from different localities can be compared with each other.

However, the exact calculation of temperatures from oxygen isotopes requires the $\delta^{18}\text{O}$ of the water be known. This is especially problematic for ancient environments, although correction factors have been proposed to overcome this obstacle (Fairbanks, 1989).

Minimum sample weight for geochemical analysis often requires a relatively large sample and, consequently, large drill holes or milled surfaces that extend over several daily increments or even

two months of growth (Goodwin et al., 2001). Furthermore, the increments in the center of drill holes are over-represented in geochemical analysis, while growth increments on the edge of drill holes contribute much less to the sampled area. Although technical advances may soon correct for these inadequacies, IWA is much cheaper and faster than geochemical approaches.

4.4. How can IWA and geochemical approaches work together for environmental reconstructions?

IWA can complement oxygen isotope analysis of Recent and fossil *Chione* specimens from other localities. IWA provides an overview of the thermal profile of the first half of the year with very high temporal resolution. Calibration with oxygen isotope analysis could then be applied to confirm or recalibrate the IWA temperature results. The combination of both methods can significantly reduce the number of geochemical measurements needed to reconstruct the intra-annual temperature profile.

Once reconstruction of daily temperatures from oxygen isotope values is possible, the effect of other factors on growth can be quantified. Differences between daily IWA temperatures and daily $\delta^{18}\text{O}$ temperatures may reflect other environmental parameters influencing growth, such as salinity or nutrient availability.

5. Conclusions

This study is the first to reconstruct daily water temperatures from intertidal bivalve mollusk growth rates. Analysis of shell growth rates of *Chione cortezi* shells can reconstruct intra-annual temperature regimes of the shallow waters in the northern Gulf of California. The data treatment includes extraction of growth trends and cycles of the daily growth increment width chronologies and the calculation of scaled growth indices. Daily water temperatures for the first half of the year can be calculated from scaled growth increments using a multi-valued function. In combination with intra-annual dating techniques based on daily increment counts, our model provides informa-

tion about how long a specific temperature range lasted and how fast water temperatures increased or decreased. The validity of this model was demonstrated for recent and subrecent *C. cortezi* specimens in the northern Gulf of California. Further studies should (1) examine additional shells at different sites for this species and (2) test the validity of this model for other mollusk species. Environmental reconstructions from growth rates can substitute for and/or complement geochemical analysis.

Acknowledgements

This study has been made possible by a post-doctoral scholarship (Lynen program) by the Alexander-von-Humboldt foundation (to B.R.S.) and NSF Grant EAR 9805165 to (K.W.F.). Skin temperature data were obtained by the NOAA-CIRES Climate Diagnostics Center, Boulder, Colorado, at <http://www.cdc.noaa.gov/>. We are grateful to S. Connolly (Department of Marine Biology, James Cook University, Townsville, Australia) for helpful discussions. We thank Douglas S. Jones, Thomas M. Marchitto Jr., Franz T. Fürsich and David J. Bottjer, and the editor Frans Koning for the thorough review of the manuscript. This is C.E.A.M. (Centro de Estudios de Almejas Muertas) publication no. 42.

References

- Bauer, G., 1992. Variation in the life span and size of the freshwater pearl mussel. *J. Anim. Ecol.* 61, 425–436.
- Berry, W.B.N., Barker, R.M., 1968. Fossil bivalve shells indicate longer month and year in Cretaceous than present. *Nature* 217, 938–939.
- Briffa, K.R., Jones, P.D., Schweingruber, F.H., Karlén, W., Shiyatov, S.G., 1996. Tree-ring variables as proxy climate indicators: problems with low-frequency signals. In: Jones, P.D., Bradley, R.S., Jouzel, J. (Eds.), *Climate Variations and Forcing Mechanisms of the Last 2000 Years*. Springer, Berlin, pp. 9–41.
- Broecker, W.S., 1989. The salinity contrast between the Atlantic and Pacific oceans during glacial time. *Paleoceanography* 4, 207–212.
- Clark, G.R., II, 1975. Periodic growth and biological rhythms in experimentally grown bivalves. In: Rosenberg, G.D., Runcorn, S.K. (Eds.), *Growth Rhythms and the History of the Earth's Rotation*. Wiley, London, pp. 103–117.
- Cook, E.R., Kairiukstis, L.A., 1990. *Methods of Dendrochronology. Applications in the Environmental Sciences*. Kluwer Academic Publishers, Dordrecht, XII +394 pp.
- Davenport, C.B., 1938. Growth lines in fossil pectens as indicators of past climates. *J. Paleontol.* 12, 514–515.
- Dolman, J., 1975. A technique for the extraction of environmental and geophysical information from growth records in invertebrates and stromatolites. In: Rosenberg, G.D., Runcorn, S.K. (Eds.), *Growth Rhythms and the History of the Earth's Rotation*. Wiley, London, pp. 191–221.
- Evans, J.W., 1972. Tidal growth increments in the cockle *Clionocardium nuttalli*. *Science* 176, 416–417.
- Fairbanks, R.G., 1989. A 17000-year glacio-eustatic sea level record: influence of glacial melting rates on the Younger Dryas event and deep-ocean circulation. *Nature* 342, 637–642.
- Fritts, H.C., 1976. *Tree Rings and Climate*. Academic Press, London, xii +567 pp.
- Goodwin, D.H., Flessa, K.W., Schöne, B.R., Dettman, D.L., 2001. Cross-calibration of daily growth increments, stable isotope variation, and temperature in the Gulf of California bivalve mollusk *Chione cortezi*: implications for paleoenvironmental analysis. *Palaios* 16, 387–398.
- Grossman, E.L., Ku, T.-L., 1986. Oxygen and carbon isotope fractionation in biogenic aragonite; temperature effects. *Chem. Geol. Isot. Geosci. Sect.* 59, 59–74.
- Gunter, G., 1957. Temperature. *Mem. Geol. Soc. Am.* 67, 159–184.
- Hastings, J.R., 1964. Climatological data for Baja California. *Tech. Rep. Meteorol. Climatol. Arid Reg.* 14, 93.
- Jones, D.S., 1996. Playing back skeletal recordings. *Palaios* 11, 293–294.
- Jones, D.S., Arthur, M.A., Allard, D.J., 1989. Sclerochronological record of temperature and growth from shells of *Mercenaria mercenaria* from Narragansett Bay, Rhode Island. *Mar. Biol.* 102, 225–234.
- Kennish, M.J., Olsson, R.K., 1975. Effects of thermal discharges on the microstructural growth of *Mercenaria mercenaria*. *Environ. Geol. (Springer)* 1, 41–64.
- Kirby, M.X., Soniat, T.M., Spero, H.J., 1998. Stable isotope sclerochronology of Pleistocene and Recent Oyster shells (*Crassostrea virginica*). *Palaios* 13, 560–569.
- Kobashi, T., Grossman, E.L., in press. Seasonality during the late Middle Eocene (ca. 39.5 Ma) indicated by *Conus tortilis* from the Moodys Branch formation, Mississippi. *Mississippi Geol.*
- Koike, H., 1980. Seasonal dating by growth-line counting of the clam, *Meretrix lusoria*. *Univ. Mus. Univ. Tokyo Bull.* 18, 1–120.
- Kowaleski, M., Goodfriend, G.A., Flessa, K.W., 1998. High-resolution estimates of temporal mixing within shell beds: the evils and virtues of time-averaging. *Paleobiology* 24, 287–304.
- Kutzbach, J.E., Guetter, P.J., 1986. The influence of changing

- orbital parameters and surface boundary conditions on climate simulations for the past 18 000 years. *J. Atmos. Sci.* 43, 1726–1759.
- Kutzbach, J.E., Guetter, P.J., Behling, P.J., Selin, R., 1993. Simulated climatic changes: results of the COHMAP climate-model experiments. In: Wright, H.E., Kutzbach, J.E., Webb, T., III, Ruddiman, W.F., Street-Perrott, F.A., Bartlein, P.J. (Eds.), *Global Climate Since the Last Glacial Maximum*. University of Minnesota Press, Minneapolis, MN, pp. 24–59.
- Lavín, M.F., Sánchez, S., 1999. On how the Colorado River affected the hydrography of the upper Gulf of California. *Cont. Shelf Res.* 19, 1545–1560.
- Marchitto, T.M., Jones, G.A., Goodfriend, G.A., Weidman, C.R., 2000. Precise temporal correlation of Holocene mollusk shells using sclerochronology. *Quat. Res.* 53, 236–246.
- Millán-Núñez, R., Santamaría-del-Ángel, E., Cajal-Medrano, R., Barocio-León, Ó.A., 1999. The Colorado River Delta: a high primary productivity ecosystem. *Cienc. Mar.* 25, 509–524.
- Neville, A.C., 1967. Daily growth layers in animals and plants. *Biol. Rev.* 42, 421–441.
- Pannella, G., MacClintock, C., 1968. Biological and environmental rhythms reflected in molluscan shell growth. *Paleontol. Soc. Mem.* 42, 64–81.
- Schöne, B.R., Goodwin, D.H., Flessa, K.W., Dettman, D.L., Roopnarine, P.D., 2002. Sclerochronology and growth of the bivalve mollusks *Chione (Chionista) fluctifraga* and *C. (Chionista) cortezi* in the northern Gulf of California, Mexico. *Veliger* 45, 45–54.
- Steuber, T., 1996. Stable isotope sclerochronology of rudist bivalves: growth rates and Late Cretaceous seasonality. *Geology* 24, 315–318.
- von Bertalanffy, L., 1934. Untersuchungen über die Gesetzmäßigkeit des Wachstums. I. Teil. *Arch. Entwickl.-Mech. Org.* 131, 616–652.
- von Bertalanffy, L., 1938. A quantitative theory of organic growth. *Hum. Biol.* 10, 181–213.
- Walford, L.A., 1946. A new graphical method for describing the growth of animals. *Biol. Bull. Mar. Biol. Lab. Woods Hole* 90, 141–147.